EXPERIMENTAL MEASUREMENT AND NUMERICAL PREDICTION OF HAIL ICE IMPACT DAMAGE ON COMPOSITE PANELS

Hyonny Kim and Keith T. Kedward

Department of Mechanical and Environmental Engineering, University of California Santa Barbara, CA, 93106, U.S.A.

SUMMARY: Hail ice impact is a realistic and yet not completely understood threat to exposed composite structures such as aircraft fuselage and wing skins, leading edge surfaces, engine nacelles, and fan blades. To investigate this threat, experiments in which carbon/epoxy composite panels were impacted by ice spheres at high velocity (30 to 200 m/s) were conducted to measure: (i) the impact energy at which damage initiates, and (ii) elastic response of the composite panel resulting from impact. Subsequent numerical analyses were performed of the impacts and were validated through correlation with experimental data. Insights gained from the numerical analyses were used to compose an analytical formula predicting the onset of delamination. This formula, based on a global energy balance, provides a cost effective (i.e. lower number of tests needed) means by which the impact damage resistance of composite structures and of composite material types can be established.

KEYWORDS: ice impact, damage resistance, delamination prediction, dynamic response.

INTRODUCTION

Thin walled composite structures subjected to severe concentrated out-of-plane loads, such as in the case of impacts, are vulnerable to the formation of damage due to the low strength these materials possess in the out-of-plane direction relative to those in-plane. While impact by metallic projectiles has been studied thoroughly [1-6], this paper addresses the issue of hail ice impacting thin composite structures at high velocity (30 to 200 m/s). The focus of the paper is on predicting the impact damage initiation, or failure threshold, for a given thickness composite panel and known level of impact threat (i.e. ice sphere diameter and velocity). The objective of this paper therefore is to present a method by which such a prediction can be achieved. Furthermore, it is argued that this is a method by which the ice impact damage resistance of any composite structure or material system can be established.

In addition to ice impact experimental results, the results of numerical simulations of ice impacts on composite panels is presented. These dynamic finite element simulations are correlated with the experiments. Fig. 1 shows the general problem, i.e. a composite panel held in an aluminum fixture subject to normal impact by hail ice at the panel center.

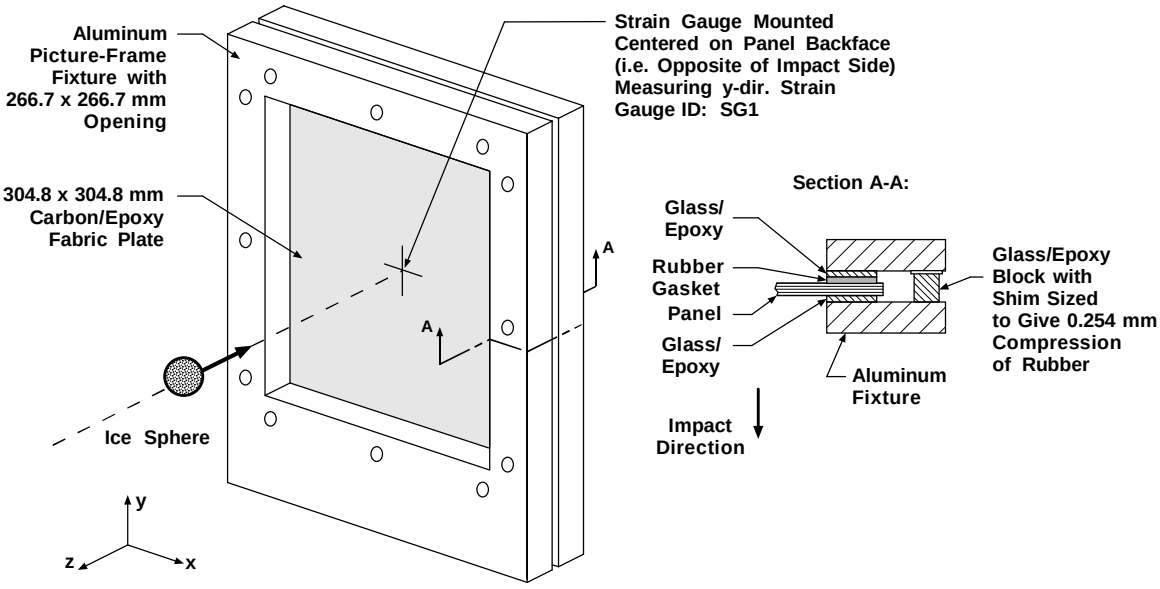

Fig. 1: Composite Panel Target and Fixture Cross Sectional Detail

EXPERIMENTS

A series of ice impact experiments have been performed to investigate: (i) the impact energy at which damage initiates, and (ii) the response of thin gauge composite panels impacted by ice. Previous work discusses these experiments in detail [7,8]. Of direct interest is the experimentally measured failure threshold energy (FTE) level. This is defined as the projectile incoming kinetic energy at which damage to the laminated carbon/epoxy fabric panels initiates. Below this kinetic energy level, impacts onto the panel targets produce no apparent damage. The failure mode observed for impacts at energy levels slightly above the FTE was delamination. This initial failure mode was also reported in the work by Elber [4].

Table 1 summarizes the experimentally measured FTE for the two panel resin types and six panel thickness values tested. The values reported refer to the projectile kinetic energy at which delamination initiates. The table shows the FTE to be dependent upon both panel thickness and ice diameter. For some panel/diameter combinations, several tests were performed using different panels (same thickness) with the same diameter ice. This produced multiple data points for the same test condition by which to ascertain the repeatability of the measured FTE data. It should be noted that the carbon/epoxy fabric panels tested all had quasi-isotropic type lay-ups, effectively resulting in bending stiffness (as calculated by laminated plate theory) which is dependent only upon thickness, much like isotropic plates.

Table 1: Failure Threshold Energy (FTE) Level for AS4/8552 and AS4/977 Panels

Panel Thick (mm)	Weave*/ Resin	Lay-Up	Failure Threshold Energy (J) for Ice Diameter: 25.4 mm	42.7 mm	50.8 mm
1.22	8HS/8552	$[0/45]_s$	56	115, 129, 119	111, 114
1.83	8HS/8552	$[0/45/90]_s$	N/A	190, 195, 202	N/A
2.44	8HS/8552	$[0/45/90/-45]_s$	95	250, 254	318
1.42	5HS/977	$[0/45/90]_s$	N/A	122	N/A
1.91	5HS/977	$[0/45/90/-45]_s$	84	199, 210	N/A
2.62	5HS/977	$[0/45/90/-45/0/\underline{45}]_s$	N/A	277	380

* Fabric weave styles: 8 HS = Eight Harness Satin, 5 HS = Five Harness Satin

The delamination failure surface morphology due to impact is rather complex. Differences in opinion currently exists among researchers [3,5,6] as to the primary cause for delamination damage formation due to transverse impacts. It is attributed to either interlaminar shear (ILS) or interlaminar tension (ILT) stress. Most likely it is a combination of both.

NUMERICAL ANALYSES

The ability to predict impact damage formation is of applied interest, especially in regard to establishing a structure's impact damage resistance capability during the design stage. The approach taken was to perform numerical finite element analysis (FEA) simulations of ice impacting composite panels to determine the stress state which is built up just prior to damage initiation. The models therefore involve a highly deformable ice projectile impacting a panel target operating in the elastic range. The general impact problem shown in Fig. 1 depicts the details of the panel boundary. The aluminum picture-frame fixture provided a nearly clamped boundary. Silicone rubber gaskets used at the panel boundary provided a uniform clamping pressure which was not so high as to restrict in-plane movement of the panel when it responded to the impact. The compliance of this gasket resulted in a boundary which was not perfectly clamped, particularly with respect to the rotation permitted at the panel boundary.

Simulations were performed using the explicit finite element code *DYNA3D* [9]. The model shown in Fig. 2 is of a 42.7 mm ice sphere impacting a 2.44 mm thick, eight ply panel. This quarter-symmetric model, having 10,284 eight-node solid elements, employs seven layers of solid elements, each having oriented orthotropic elastic properties, to model the laminated plate. Solid elements were used instead of shell elements due to the shell element's inability to exactly calculate through-the-thickness stress components. These through-the-thickness, or interlaminar in the case of laminated composites, stress components are essential for the prediction of the delamination failure mode. The model incorporates the previously developed impact ice material model developed by Kim and Kedward [8] for which material input parameters used by the code *DYNA3D* are listed in Table 2. Lamina orthotropic elastic properties used to model the composite are provided in Table 3. The ice sphere was given only a velocity initial condition, thus relying on the defined contact surfaces to account for the sphere-to-panel interaction. Note in Fig. 2 that the details of the panel boundary, i.e. the silicone rubber gasket and glass/epoxy blocks, with frictional sliding interfaces, needed to be modeled in order to correctly predict the long-term panel center deflection history response.

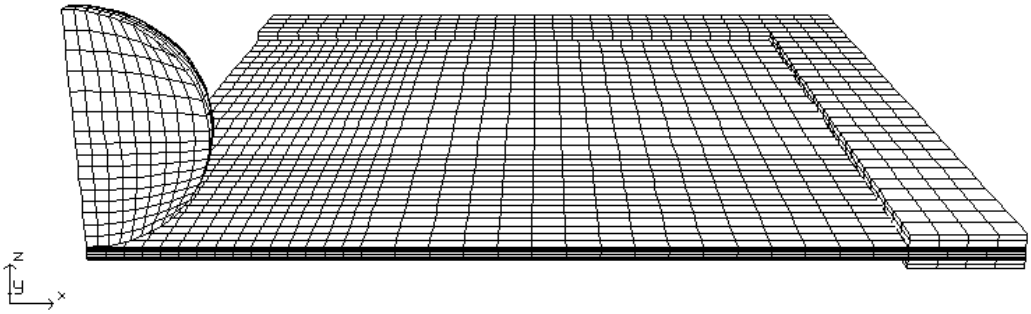

Fig. 2: DYNA3D Mesh of 42.7 mm Diameter Ice Impacting 2.44 mm Thick Composite Panel

Two experimental test cases simulated using *DYNA3D* are summarized in Table 4. Listed for each case are the measured peak strain and the time to reach peak strain. The strain gauge, labeled as SG1, is located at the panel center, exactly opposite of the impact location (see Fig. 1). The *DYNA3D* models used for simulating these tests are also listed in the table.

Table 2: Ice Material Input for DYNA3D "Material Type 13 Elastic-Plastic with Failure" Model

Property	Value
Density	846 kg/m^3
Elastic Shear Modulus	3.46 Gpa
Yield Strength	10.3 Mpa
Hardening Modulus	6.89 Gpa
Bulk Modulus	8.99 Gpa
Plastic Failure Strain	0.35 %
Tensile Failure Pressure †	- 4.00 Mpa

† Negative value input denotes hydrostatic tension.

Table 3: AS4/8552 Eight Harness Satin Fabric Lamina Mechanical Properties Used to Model Each Orthotropic Layer

E_{11} = 71.7 Gpa	E_{22} = 69.5 Gpa	E_{33} = 6.89 Gpa
G_{12} = 5.17 Gpa	G_{23} = 5.17 Gpa	G_{13} = 5.17 Gpa
ν_{21} = 0.038	ν_{31} = 0.029	ν_{32} = 0.030

E_{11}, E_{22}, G_{12}, and ν_{21} are measured properties; E_{33}, G_{23}, and G_{13} are approximate. Density = 1,506 kg/m^3.

Table 4: Experimental Test Cases Simulated by DYNA3D

Test No.	Ice Dia. (mm)	Velocity (m/s)	Kinetic Energy (J)	Test Result	Peak Strain, SG1 (με)	Time to Peak (μsec.)	*DYNA3D* Model ID
137	42.7	73	95	No Damage	10,350	77	pan15b
138	25.4	154	84	No Damage	11,870	74	pan18c

Correlation of simulation with the experimentally measured panel center deflection history is shown in Fig. 3 for test case 137. While the displacement history is predicted closely by *DYNA3D* only for the first half of the oscillation, it is within this time scale in which stress and strain components contributing to the prediction of panel failure are of significant magnitude. The times at which predicted bending strain and ILS stress are maximum are indicated in the enlarged time scale portion of Fig. 3.

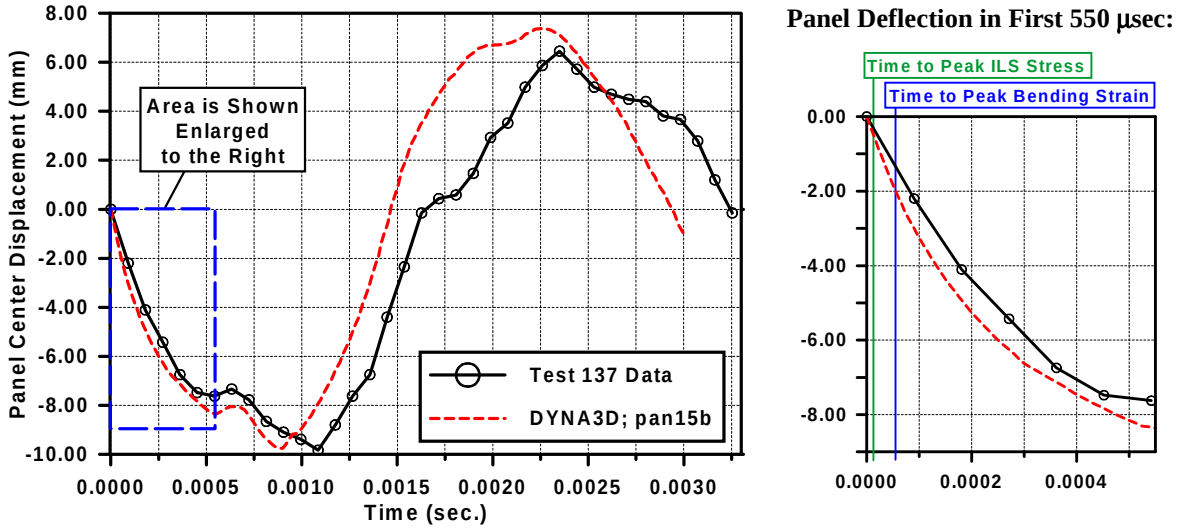

Fig. 3: Comparison of Predicted to Measured Panel Center Deflection History

The predicted strain at the center of the panel is compared with the measured data of each test. Fig. 4 shows the *DYNA3D* simulation "pan15b" compared with test data up to 2.0 msec., while in Fig. 5, the model "pan18c" prediction is compared with test data to a time of 0.7 msec. As seen in the figures, the *DYNA3D* models predict the center strain gauge SG1 history quite well for both cases. The peak strain, time to peak, and general overall trend matches the experimentally measured strain history. The ability to closely predict the measured strain data serves as a validation of the modeling fidelity. Now the model can be used to observe other components of strain and stress which are impossible to measure experimentally. In particular, the ILS stress during the impact event can be obtained using the numerical models.

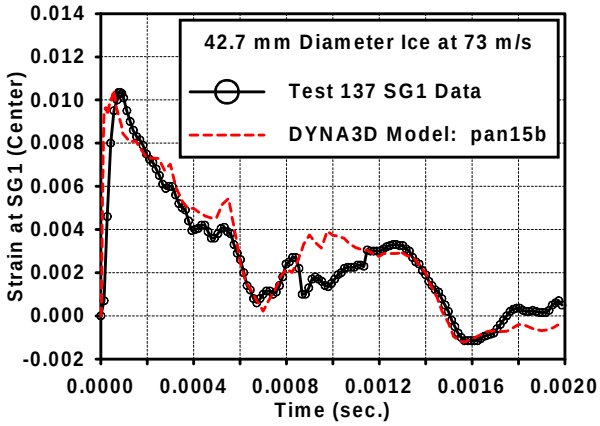

Fig. 4: Predicted Strain History at Panel Center and Measured Data for Test 137

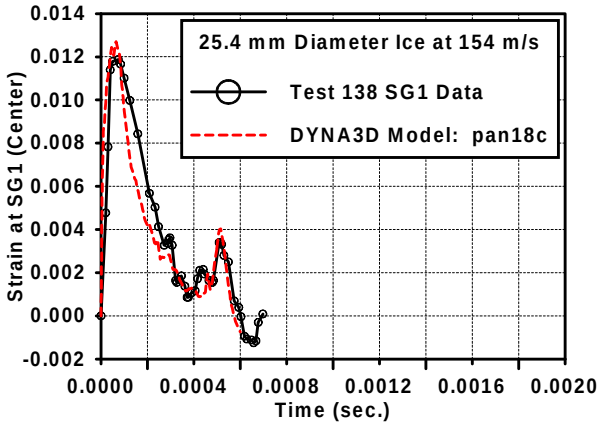

Fig. 5: Predicted Strain History at Panel Center and Measured Data for Test 138

ILS stress is considered here to be the primary driving force for the formation of impact induced delamination [3]. Fig. 6 shows the predicted peak ILS stress component τ_{xz} as a function of time for both *DYNA3D* models. This is the maximum value of shear stress in any one of the elements used to model the composite panel at each time step during the simulation. Thus the profiles in Fig. 6 are not the τ_{xz} histories of a single element, but of the particular element having the peak τ_{xz} at a given time. Note the order of magnitude difference in time scale between Fig. 6 and Figs. 4 and 5. The ILS stress τ_{xz} peaks at a time which is several times less than the time to achieve peak surface strain.

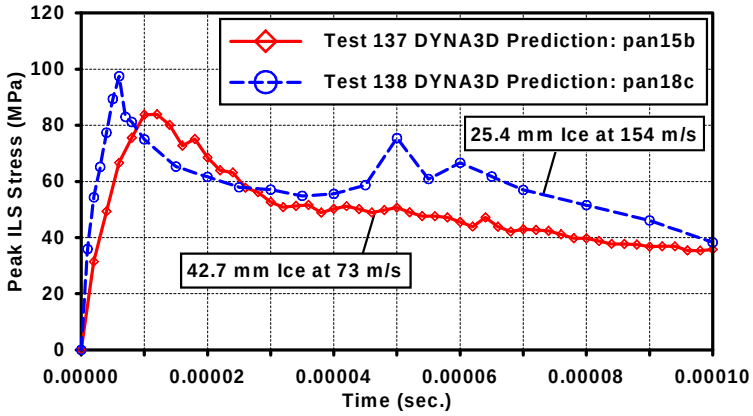

Fig. 6: Peak Interlaminar Shear (ILS) Stress τ_{xz} History for Two Simulations

Fig. 7a shows a close-up view of the sphere impacting onto the composite panel for model "pan15b" simulating Test 137. The figure displays contours of τ_{xz} at a time during which peak τ_{xz} occurs (12 μsec.). A dark triangle points out the location of the peak τ_{xz} stress. Contour plots (not shown) of τ_{xz} at time steps prior to and following the maximum allow the observation that the peak τ_{xz} stress moves outwards, away from the center of the plate as time progresses. This stress is always a maximum at the boundary of the contact patch which the ice makes as it crushes onto the panel. Another observation to note is the through-thickness location of the maximum shear stress. During the time scale in which τ_{xz} is a maximum, the through-the-thickness profile of τ_{xz} of is close to parabolic, with the peak stress located halfway through the panel thickness.

Fig. 7b shows a plot of τ_{xz} through the panel thickness at the time of peak τ_{xz} as predicted by the *DYNA3D* model "pan15b." This profile is at a location 5.1 mm from the plate center, corresponding with the location pointed out in Fig. 7a. Also plotted is a parabolic curve fit,

based on matching the peak stress, which shows the through-thickness profile of τ_{xz} to be quite nearly parabolic. Thus the parabolic transverse shear stress profile often assumed in shear deformation beam and plate theory is justified as a good approximation, even for this complex impact problem. Fig. 7c shows the profile of τ_{xz} through the thickness of the panel for the model "pan18c." Similar to Fig. 7b of model "pan15b," the content of this figure reaffirms that the ILS stress profile can be well approximated by an assumed parabolic function.

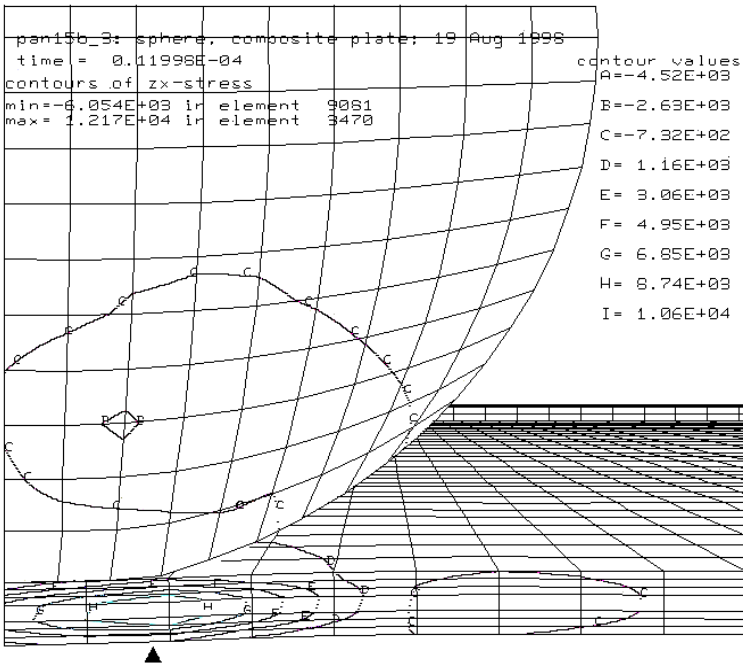

(a)

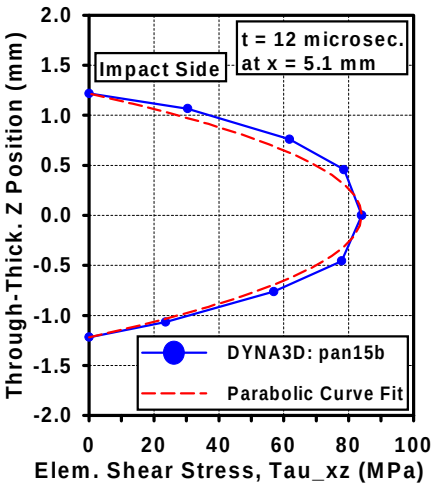

(b)

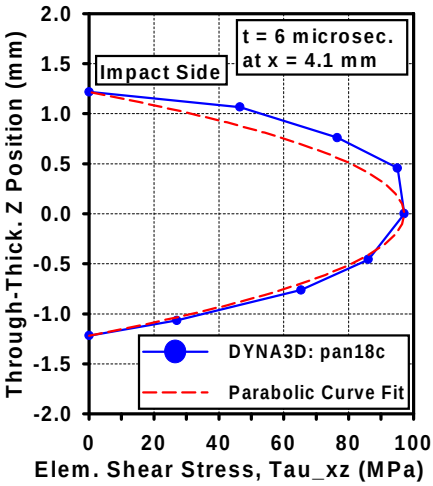

(c)

Fig. 7: (a) DYNA3D Model "pan15b" Contour Plot of τ_{xz} at time t = 12 μsec., Max. τ_{xz} = 83.9 Mpa (12,170 psi);

(b) DYNA3D Model "pan15b" τ_{xz} Profile Through Panel Thickness at Time of Peak Stress (t = 12 μsec.); 42.7 mm Ice at 73 m/s;

(c) DYNA3D Model "pan18c" τ_{xz} Profile Through Panel Thickness at Time of Peak Stress (t = 6 μsec.); 25.4 mm Ice at 154 m/s

Fig. 8 shows the profile of τ_{xz} as a function of position away from the impact location, or panel center, at the time of peak τ_{xz} stress. The stress is taken from elements at the mid-depth location along the symmetry plane defined by the *x* and *z* axes (see Fig. 2 for axes definition). In Fig. 8, the results of both *DYNA3D* models show τ_{xz} to be quite localized near the location of impact during the time in which peak τ_{xz} occurs. Beyond 25 mm distance from the impact location, τ_{xz} is zero. Note that the panel boundaries are at 133.4 mm distance away from the impact location, and thus at the time of peak τ_{xz} the panel boundaries are not yet aware of the presence of the impacting ice sphere.

Table 5 is a summary of the results for *DYNA3D* models "pan15b" and "pan18c." Listed are the numerically predicted peak τ_{xz} and peak surface strain at the location SG1 (panel backside center) along with the times to peak τ_{xz} and peak surface strain. Comparison of these times

emphasizes that the ILS stress, τ_{xz}, peaks well before the primarily bending induced surface strain. In other words, the panel will always experience an interlaminar failure, such as delamination, before fiber failure. This sequence of material failure progression during impacts, i.e. shear failure before bending induced fiber failure, was also reported by Elber [4].

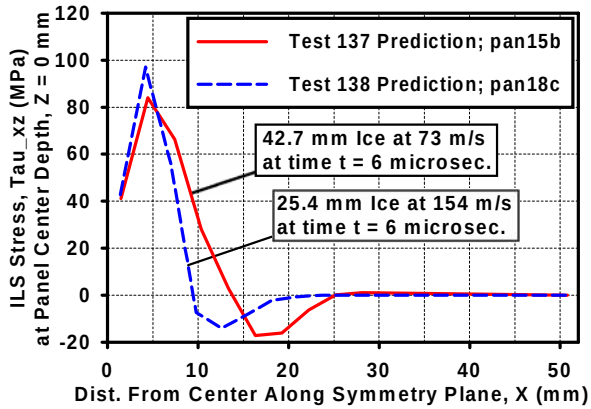

Fig. 8: ILS Stress τ_{xz} as a Function of Distance from Impact Location, x

Table 5: DYNA3D Models Results Summary

***DYNA3D* Model ID**	**Peak τ_{xz}** (MPa)	**Time to Peak** (μsec.)	**Peak Surface Strain** (με)	**Time to Peak** (μsec.)
pan15b‡	83.9	12	10,430	54
pan18c	97.5	6	12,700	65

‡ see times for model "pan15b" illustrated in Fig. 3

FAILURE THRESHOLD ENERGY LEVEL PREDICTION

The numerical models have shown that the ILS stress peaks at a time well in advance of the time needed to develop maximum bending strain on the surface of the plate, thus indicating delamination to be the initial failure mode once the failure threshold energy (FTE) level is exceeded; this observation confirms the author's experimental findings [7,8]. A global energy balance was performed on the system to establish a relationship between the FTE and the experimental parameters. Fig. 9 depicts the plate impact problem at a state just before impact and at a state early on during the impact event, specifically at the time during which peak ILS stress occurs. Just before impact, State 1, the only energy in the system is the kinetic energy, T_1, of the ice sphere of mass m which travels at an initial velocity v_o (see Eqn 1) . During the impact event, State 2, the ice (still having mass m) is at a reduced velocity v which is expressed as a proportion of the initial velocity, i.e. $v = \alpha v_o$ $(0 < \alpha < 1)$. At State 2, the total energy in the system (see Eqn 2) is a combination of the sphere's remaining kinetic energy plus the energy stored by elastic deformations in the plate and ice sphere. V_{shear} is the energy due to shear deformation of the plate. V_{other} accounts for the other sources of elastic energy storage such as the bending and membrane deformation in the plate, and the elastic energy stored in the ice sphere.

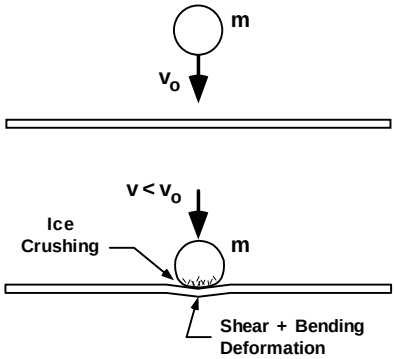

State 1:

$$E_1 = T_1 = \tfrac{1}{2} m v_o^2 \qquad (1)$$

State 2:

$$E_2 = T_2 + V_2 = \tfrac{1}{2} m v^2 + V_{shear} + V_{other} \qquad (2)$$

Fig. 9: Energy Balance for Plate Impact Problem

An energy balance can now be written using Eqns (1) and (2):

$$E_2 - E_1 = W_{nc} \tag{3}$$

where W_{nc} is the non-conservative work which occurs in passing from State 1 to State 2. This term is primarily the work performed due to the local crushing of the ice sphere near the location of sphere-to-panel contact. It also accounts for energy loss due to friction. The strain energy due to shear deformation can be expressed using a volume integral over the portion of the plate in which shear deformation occurs. From the *DYNA3D* models, it has been shown that during the time frame in which peak ILS stress develops, the panel deformations are quite localized near the point of impact (see Fig. 3). Calculation of the shear deformation energy is difficult due to the complex distribution τ_{xz} has through the panel thickness and the in-plane coordinates, the latter distribution being shown in Fig. 10 along the panel center-depth location. A simplifying approximation can be made by assuming an average value of shear stress, $\tau_{ave.}$, throughout the volume of panel which is affected by the sphere impact. This allows for a simple relationship for the shear strain energy to be composed.

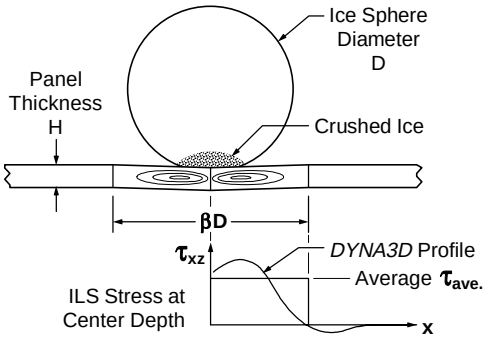

Fig. 10: Panel Shear Deformation and ILS Stress Profile

$$V_{shear} = \tfrac{1}{2}\int_{Vol.} \frac{\tau_{xz}^2}{G_{xz}} dVol. = \frac{\tau_{ave.}^2}{2G_{xz}} \pi H \left(\frac{\beta D}{2}\right)^2 \tag{4}$$

where:
- $\tau_{ave.}$ = average shear stress
- G_{xy} = interlaminar shear modulus of composite panel
- βD = diameter of volume having non-zero shear stress (β is a proportionality constant, $0 < \beta < 1$)

Volume of plug is simply: $Vol. = \pi H \left(\frac{\beta D}{2}\right)^2$.

Substituting Eqns 1, 2, and 4 into Eqn 3, making the previously stated substitution of $v = \alpha v_o$, and recognizing that the initial kinetic energy, $KE_o = \frac{1}{2} m v_o^2$, the energy balance can now be rewritten as:

$$KE_o = \frac{1}{1-\alpha^2}\left[\frac{\tau_{ave.}^2}{8G_{xy}} \pi \beta^2 D^2 H + V_{other} - W_{nc}\right] \tag{5}$$

Within the time scale to which the ILS stress peaks, it shall be assumed that the terms V_{other} and W_{nc} are small compared to the magnitudes of the shear deformation energy and kinetic energy terms. These terms can be considered as constants due to their minor contributions, despite the fact that there must be some functional dependence of these variables on the geometric parameters *H* and *D*. Observing Eqn. 5, α and β are both proportionality constants, indicators of the amount of sphere deformation and velocity reduction. The only controllable experimental parameters remaining which would relate the kinetic energy to the average shear stress are panel thickness *H* and sphere diameter *D*. Finally, consider the case in which the projectile has enough initial kinetic energy to initiate a delamination failure. The average shear stress would be at some critical value, $\tau_{ave.}^{crit.}$, and the kinetic energy, KE_o, would be the previously discussed failure threshold energy, FTE. Making these substitutions into Eqn 5,

$$FTE = \frac{1}{1-\alpha^2}\left[\frac{\left(\tau_{ave.}^{crit.}\right)^2}{8G_{xy}} \pi \beta^2 D^2 H + V_{other} - W_{nc}\right] = C_1 + C_2 D^2 H \tag{6}$$

The parameters C_1 and C_2 can be empirically determined. Eqn 6 establishes the functional form in which FTE is related to the geometric parameters *H* and *D*. The data in Table 1 are plotted in Fig. 11 in accordance to Eqn 6 (i.e. FTE versus D^2H). All of the experimental data collapses under this single relationship for the entire range of test conditions. The linear fit to the data, following the form of Eqn 6, indicates that C_1 and C_2 in Eqn 6 are independent of *D* and *H*, and are empirically determined constants over the range of ice impact velocities tested. Having established this functional relationship, the FTE can be predicted for any combination of ice diameter and panel thickness, within the requirement that the impact occurs at high velocity, and the ice sphere fails in a similar manner as tested.

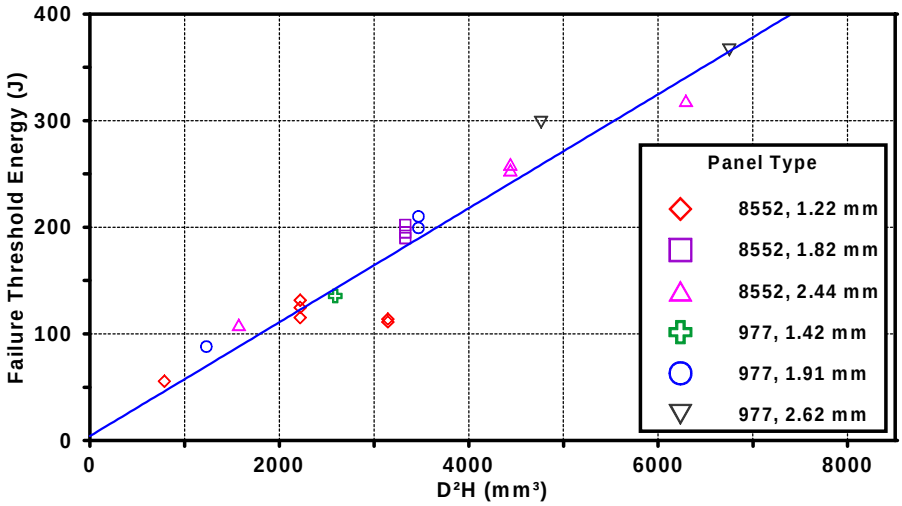

Fig. 11: Summary of Panel Failure Threshold Energy for All Tests

CONCLUSIONS

Experimental studies into the high velocity impact of thin gauge composite panels by simulated hail ice have found that there exists a failure threshold energy (FTE) level. Delaminations were identified by experiments and analysis to be the initial failure mode to occur for impacts at levels slightly above the FTE. At energy levels well beyond the FTE, other failure modes involving fiber failure would occur. The formation of delaminations is considered within this body of research to be primarily caused by excessive interlaminar shear (ILS) stresses. Numerical finite element analysis (FEA) models simulating the experimental cases of non-damaging impacts onto composite panels show that the ILS stress approaches levels just below the ILS strength of the tested material (117 to 125 MPa). This stress is a maximum almost immediately after impact. The time to reach peak ILS stress (causes delamination) occurs several times earlier than the time to reach peak bending strain (causes fiber failure). Thus the models reinforce the previous experimental observations that delamination failures occur before bending induced fiber failure.

The numerical modeling results assisted in making assumptions and simplifications in the formulation of an energy balance relationship which predicts the FTE as a function of geometric experimental parameters. The experimentally measured FTE data, when plotted in accordance to the functional form of this relationship, indicated a linear relationship between the FTE and the grouping of geometric parameters D^2H. In other words, the assumptions made in the relationship's formulation captured the fundamental behavior of this impact damage initiation problem (i.e. all data collapsed into a single trend), leaving only two

constants which can be determined empirically. Once determined, the form of this relationship can then be applied to establish the ice impact damage resistance for any material system using a relatively low number of tests. Furthermore, due to the time scale within which the ILS stress peaks, panel deflections remain quite localized. The relationship is therefore independent of panel boundary conditions and can be directly applied to predicting damage initiation in composite structures of similar gauge thickness when impacted by ice at high velocities. Finally, it is proposed that the method presented employing the energy based analysis can be applicable to other forms of impact as well as ice, such as impacts by metallic projectiles. Further work is needed however in order to verify this hypothesis.

ACKNOWLEDGEMENTS

Acknowledgement to United Technologies Pratt & Whitney for funding this research through a DARPA sponsored Technology Reinvestment Project. All *DYNA3D* computations were run on the National Partnership for Advanced Computational Infrastructure (NPACI) San Diego Supercomputer Center (SDSC) Cray T90.

REFERENCES

1. Jackson, W. C., and Poe, C. C. Jr., "The Use of Impact Force as a Scale Parameter for the Impact Response of Composite Laminates," NASA Technical Memorandum 104189, AVSCOM Technical Report 92-B-001, January 1992.

2. Shivakumar, K. N., Elber, W., and Illg, W., "Prediction of Impact Force and Duration Due to Low-Velocity Impact on Circular Composite Laminates," *Transactions of the ASME*, September 1985, Vol. 52, pp. 674-680.

3. Joshi, S. P. & Sun, C. T., Impact induced fracture in a quasi-isotropic laminate. *Journal of Composites Technology and Research*, Vol. 9, 1987 40-46.

4. Elber, W., "The Effect of Matrix and Fiber Properties on Impact Resistance," *Tough Composite Materials*, NASA Conference Publication, Noyes Publishing, Park Ridge, NJ, 1985, pp. 89-110.

5. Clark, G., "Modelling of Impact Damage in Composite Laminates," *Composites*, Vol. 20, No. 3, May 1989, pp. 209-214.

6. Wu, H.-Y. T. & Springer, G. S., "Impact Induced Stresses, Strains, and Delaminations in Composite Plates," *Journal of Composite Materials*, Vol. 22, June 1988, pp. 533-560.

7. Kim, H., and Welch, D. A., "Investigation of Hail Ice Impact on Composite Structures," Pratt & Whitney Technical Report, EII No. 95-200-0035-B, ACP/Pratt & Whitney Proprietary, June 1, 1995.

8. Kim, H. and Kedward, K. T., "Experimental and Numerical Analysis Correlation of Hail Ice Impacting Composite Structures," AIAA-99-1366, *40th AIAA / ASME / ASCE / AHS / ASC Structures, Structural Dynamics, and Materials (SDM)* Conference, April 12-15, 1999, St. Louis, MO.

9. Whirley, R. G., and Engelmann, B. E., "DYNA3D A Nonlinear, Explicit, Three-Dimensional Finite Element Code For Solid and Structural Mechanics – User Manual," Lawrence Livermore National Laboratory, UCRL-MA-107254 Rev. 1, November 1993.